C-1.3.1   Development of the Transport, Transformation and Removal Model for Acidic and Oxidative Pollutants in the East Asia(Final Report)

Contact Person   Kentaro Murano
                  Senior Research Scientist
                  Global Environment Division
                  National Institute for Environmental Studies
                  16-2 Onogawa, Tsukuba, Ibaraki 305, Japan
                  Phone +81-0298-50-2537   Fax +81-0298-51-4732

The spectral limited area model was nested within the grid model (FLM) used formerly by spectral boundary coupling method to gain higher spatial resolution over focused area while keeping wider model domain. Meteorological model was also improved to be able to output cloud water content in order to calculate the interaction process with pollutants. Based on these data set, the Long-range Transport Model (MRI-LTM) was improved including the additional interaction process between pollutants and cloud. A numerical simulation of transport and removal of sulfur oxides in the East Asian region was performed for whole year of 1985, and adequate results were obtained.

3-D atmospheric transport model which includes chemical reactions, the STEM (Sulfate Transport Eulerian Model), was also applied to the east Asia region. The STEM model successfully simulated the typical time variation of observed concentrations. It was found that wind pattern variations associated with a synoptic scale pressure system are extremely important for the transport of pollutants.

Key words   Numerical Model, Nesting, Sulfur Oxides, Transformation, Deposition

1. Introduction

Recently, the region of East Asia is characterized by high and growing population density and, in some regions intensive, rapid industrialization. As a natural consequence, energy is being consumed in enormous quantities in the region. More than 24 million tonnes/year of anthropogenic sulfur oxides are emitted into the atmosphere, and about 70% of this value is predominated by emission sources in China. Thus acid deposition originated in continental emission sources is becoming a serious problem in the East Asian region.

The spatial distribution of concentrations for ozone, sulfur dioxide and nitrogen oxides were fragmentarily obtained by intensive aircraft observations over the East China Sea, the Yellow Sea, and the Sea of Japan[1]. In East Asia, however, no systematic monitoring network for acid deposition have been set up. Therefore it is very difficult to estimate the amounts of acid deposition in this region. One way to circumvent this difficulty is by using numerical models. By using numerical long-range transport model developed by the Meteorological Research Institute (the MRI Long-range Transport Model: MRI-LTM), the impact on acid deposition at several receptors in Japan originating continental emissions was evaluated[2]. The MRI-LTM does not include in-cloud scavenging process, because of the clouds are not captured by the meteorological model including the MRI-LTM with a horizontal resolution of 127 km. It have been said that the in-cloud scavenging process plays important role in wet deposition[3],[4]. In order to include this process, therefore, the MRI-LTM was improved to gain higher spatial resolution.

2. Outline of the Model Results (Meterological Research Insititue)

The MRI–LTM consists of two main submodels; a meteorological model which predicts meteorological variables, and dispersion model which includes advection, diffusion, deposition and chemical transformation of SO_2 to SO_4^{2-}.

2.1 Meteorological prediction submodel

Two meteorological models are combined to gain high spatial resolution over focused area; the Japan Meteorological Agency's (JMA) operational spectral limited area model around Japan (JSM) is nested in the modified fine mesh limited area model over Asian region (FLM), which is old version of operational weather forecast model of JMA. The nesting method is used the spectral boundary coupling[5].

a) Outer model

The improved FLM is used for outer model. The vertical resolution and the physical precesses of the FLM have been modified. The improved FLM has 16 layers, and the closure model of level 2[6] is employed to represent the vertical turbulent diffusion. At the lowest layer, Monin–Obukhov's similarity theory is applied to determine vertical fluxes from the ground surface. Since the detailed explanation of outer model is described[7], here, only outline of the outer model is given.

The basic equations are the primitive equations for momentum, mass, specific humidity, and virtual temperature using flux forms by using σ–coordinates on a polar stereographic projection plane at 60°N using the following set of prognostic variables:

$$u, v, \theta, q \text{ and } \pi$$

where, u and v are components of wind for x and y directions respectively, θ the potential temperature, q the specific humidity, and π is pressure at the surface.

The initial and boundary values of the outer model is given by global analysis data sets (GANL) which is developed by the Numerical Prediction Division in the Japan Meteorological Agency (JMA) to create initial conditions for the global scale weather forecast model.

The calculation domain of the model is about 9300 × 7000 km², the model domain and the topography in the model are shown in Fig. 1. The domain is horizontally covered by the Arakawa's B grid with 73×55 grid nodes, and the grid size is 127 km at 60°N.

Two types of the parametarization for precipitation is used in the model; the large scale condensation parametarization and the moist convective adjustment. The former prevents supersaturation and the latter keeps the atmospheric temperature lapse rate between the dry adiabatic and the moist adiabatic lapse rate.

Fig. 1. Domain and topography of the outer model. Inner flame indicates the area of the nested inner model.

b) Inner model

A spectral limited area model (JSM) is used for inner nested model whose spectral representation is the same as Tatsumi[8]. The JSM is fundamentally similar to the FLM except for model domain, horizontal and vertical resolution and a few physical processes. The most dissimilar point is not only spatial
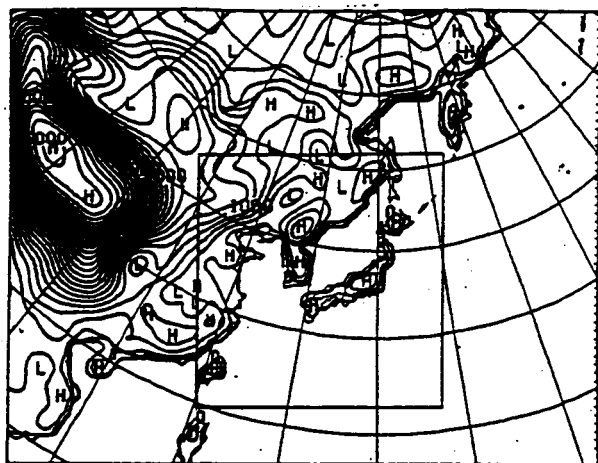
.resolution but also radiation process. Radiation process in the JSM is considered only to calculate the net radiation at the ground surface.

The JSM has a regular 97 × 97 square transform grid with a grid distance of 40 km at 60°N on a polar stereographic projection plane. The model also uses σ-coordinate system and has 19 layers in the vertical, which resolution is finer in the boundary layer near the surface.

The cloud amount are determined using relative humidity at each layer by the empirical formula[9].

2.2 Dispersion submodel

The dispersion submodel for sulfur oxides is fundamentally based on the mass conservation of sulfur oxides.

Advection and diffusion of these chemical species are described by a Lagrangian particle with random-walk model in the same coordinate system as in the meteorological submodel. The behavior of particle indicates higher resolution by interpolation of meteorological variables. Winds, precipitation and turbulent diffusivity used dispersion model are predicted by the nested meteorological submodel. The variables on each grid nodes are stored at every one hour integration of the meteorological submodel.

a) Advection and diffusion

The three-dimensional movement of a particle is calculated using the following equations:

$$\frac{dX}{dt}=u; \quad \frac{dY}{dt}=v; \quad \frac{d\sigma}{dt}=\dot{\sigma}+R \tag{1}$$

where, X, Y, and σ are positions of a particle in a three-dimensional coordinate system. A random force captured an additional displacement of a particle corresponding to vertical turbulent diffusion R is defined as:

$$R=\pm\sqrt{2K_z\delta t} \tag{2}$$

where, K_z the vertical turbulent diffusivity derived from the meteorological submodel, δt is the time step in the random-walk model, and the sign is chosen randomly for each particle and each time step.

A simplified Runge-Kutta scheme is employed for time integration of three-dimensional advection terms with a long time step $\delta t=10$ min for the outer domain. The Euler-backward scheme is employed for random vertical diffusion terms with shorter time step $\delta t=2$ min in order to avoid artificial convergence or divergence of particles at the layer where K_z varies abruptly. Each time step in the inner domain is decreased to 2/3 of the outer domain.

b) Deposition

A particle is assumed to be deposited by a dry process if following two conditions are satisfied; the height of a particle is lower than a prescribed critical height $H_d=0.99$ in σ-coordinate, and a number given randomly for each particle and each time step is smaller than a value P_d defined as

$$P_d=\frac{V_d\delta t}{H_d} \tag{3}$$

where, V_d is the dry deposition velocity. The dry deposition velocity varies with meteorological condition and underlying ground surface. The values of dry deposition velocities over several ground surface conditions are suggested[10]. On the other hand, it is

also shown that the dry deposition velocities for SO_2, SO_4^{2-}, and NO_3 vary with type of ground surface[11]. The simple assumption, therefore, is made as the dry deposition velocity of SO_2 and SO_4^{2-} varies only with two kinds of the ground surface conditions.

Wet deposition of the pollutants due to precipitation was estimated every one hour in the outer domain and 40 min in the inner domain. The particles are deposited on the ground surface with a probability of

$$P_{wd}=D_{wd}dt \cdot RR \qquad (4)$$

where, D_{wd} is the below cloud scavenging rate, dt the estimated duration of wet deposition (one hour and 40 min in the respective domain) and RR is a precipitation factor.

The precipitation factor RR is defined as;

•for particles at grid nodes
$RR=1$ if the predicted precipitation rate is exceeds a prescribed threshold value.
$RR=0$ otherwise,
•for particles between grid nodes
RR is interpolated horizontally using RRs around the particle.

Below cloud scavenging rate have been suggested in several studies[12),13)], however, values are widely scattered between 10^{-5}/sec and 10^{-3}/sec. Therefore, they are assumed in present study to be $C_{wd}=3\times10^{-5}$/sec for SO_2, and $C_{wd}=1\times10^{-4}$/sec for SO_4^{2-} for precipitation rates larger than threshold value.

c) Transformation of SO_2 to SO_4^{2-}

The only chemical transformation in this model is that of SO_2 to SO_4^{2-}, because it is very difficult to include the detailed chemical reaction of pollutants in the Lagrangian particle model. The two kinds of transformation rates are considered, one in the ambient atmosphere, the other in aqueous phase as in the cloud water. These values are arbitrarily chosen from the studies in literature. The transformation rate in the ambient atmosphere spread a range of over an order of magnitude. For example, Cox[14] estimates 0.01~0.1/hour in an urban plume for photo-oxidation with NO_x and hydrocarbons, or thermal oxidation with ozone and olefin. Eliassen and Saltbones[15] estimate a transformation rate of about 0.007/hour. The estimation by Alkezweeny and Powell[16] from atmospheric concentration data measured by air craft yield 0.10~0.12/hour. Meagher and Bailey[17] demonstrated the seasonal variation of SO_2 oxidation varying from a winter low of 0.0015/h to a summer high of 0.013. After due consideration of these values, a rate of 0.01/hour was adopted in the present model.

2.3 Verification of Inner Boundary Effect

In order to verify the effect of the spectral nesting method on the calculation of long-range transport of pollutants, a test simulation is performed in case of the Chernobyl nuclear power plant accident and the results are compared to the observation in Europe. As the observation data, the data distributed in the ATMES workshop[18] are used.

To examine the behavior of particles around the nesting inner boundary, the emission source of the particles is located in the outside of the inner domain. Figure 2 shows simulated distribution of I^{131} in the air
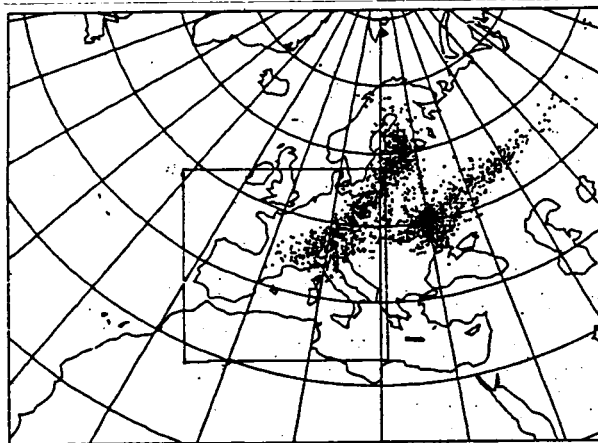

Fig. 2 Simulated distribution of I^{131} in the air at 00 UTC 1, May 1986. Inner flame indicates the area of the inner model.

at 00 UTC on May 1st, 1986, and indicates that particles flow from outer domain to inner domain without significant problem around the nested boundary.

Next, the evaluations of the nesting model are statistically performed by the following 4 cases.

- only outer model is used, averaged concentration is calculated over 254×254 km (case 1),
- only outer model is used, averaged concentration is calculated over 80×80 km (case 2),
- inner model is nested, averaged concentration is calculated over 254×254 km (case 3),
- inner model is nested, averaged concentration is calculated over 80×80 km (case 4).

The averaged time is 24 hours running mean. The score analysis is made to investigate predictability of the nested model. The threat score shows the rate of hit event. The bias score is an aim whether width of hit area is appropriate. The results are shown in Table 2.

Table 1. Root mean square error and number of hit, no-hit and false alarm of model for I[131] over Europe.

Case	RMSE	Hit	No-hit	FA
1	0.99	348	129	4
2	0.87	277	203	1
3	0.91	397	76	8
4	0.82	314	165	2

It is found in this table that nested model has higher score than non-nested model (outer model only) in threat and bias scores. Comparing the different averaged areas, RMSE in the models with 80 km square averaging area.(case 2 and case 4) are smaller than with 254 km area(case 1 and case 3), although threat score in the models with 254 km square averaging area are higher with 80 km area. Furthermore, false alarm rates in the models with narrower averaging area are higher. This indicates that narrower averaging area represents more locality and predicts better concentration of pollutants at the costs of increasing bias score.

2.4 Application to the East Asian Region

By using the nested transport model, the simulation of transport process of sulfur oxides over the East Asian region was performed for whole year of 1985. In order to create the meteorological data sets, nested meteorological submodel was used. The output meteorological variables were as follows; 3-dimensional winds, cloud water content, precipitation index, turbulent diffusivities, and geopotential. This calculation required large cpu-time, for example, it needs about 2 hours for cpu-time to predict 5 days by SX-3/14 super computer system.

The anthropogenic emission inventory of sulfur oxides for 25 Asian countries east of Afghanistan and Pakistan have been calculated for the year 1975, 1980, 1985, and 1987 base on the fuel consumption[19]. In addition to the 25 whole countries, province and region-based calculations were made for China and India. The emission inventories based on 1985's were
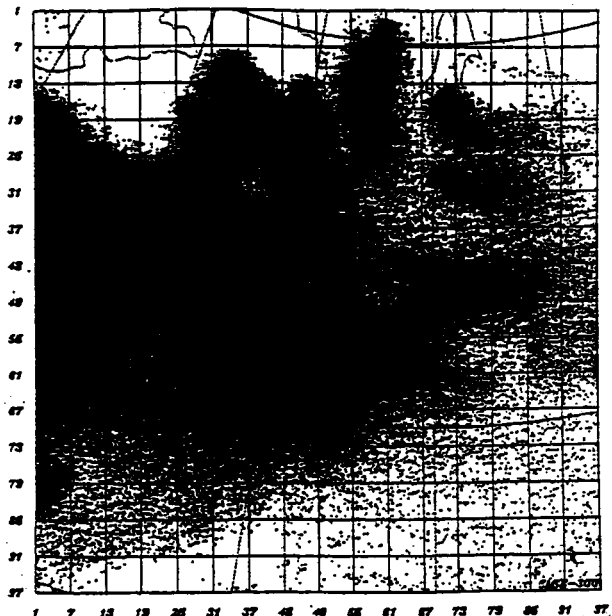

Fig. 3 The distribution of sulfur oxides in the atmosphere during 5 days from 20 Jan. to 24 Jan. 1985.

redistributed to 80 point sources based on industrial activities and population of the major cities[20]. This 80 point source emissions of sulfur oxides in the East Asia are used in this application run. The 80 point sources include emissions at Japan and Far East of Russia but for volcanic and other natural emission sources.   Figure 3 shows the horizontal distribution of sulfur oxides in the atmosphere emitted from 80 point sources in the East Asia during 5 days from 20th to 24th January, 1985. It is seen that sulfur oxides covers whole region of the East Asia in the period of only 5 days. Furthermore, dry deposition of sulfur oxides in the same period is shown in Fig. 4(a). The remarkable dry deposition occurs relatively nearby the emission sources. The wet deposition distribute widely in the downwind direction form the emission sources as seen in Fig. 4(b).
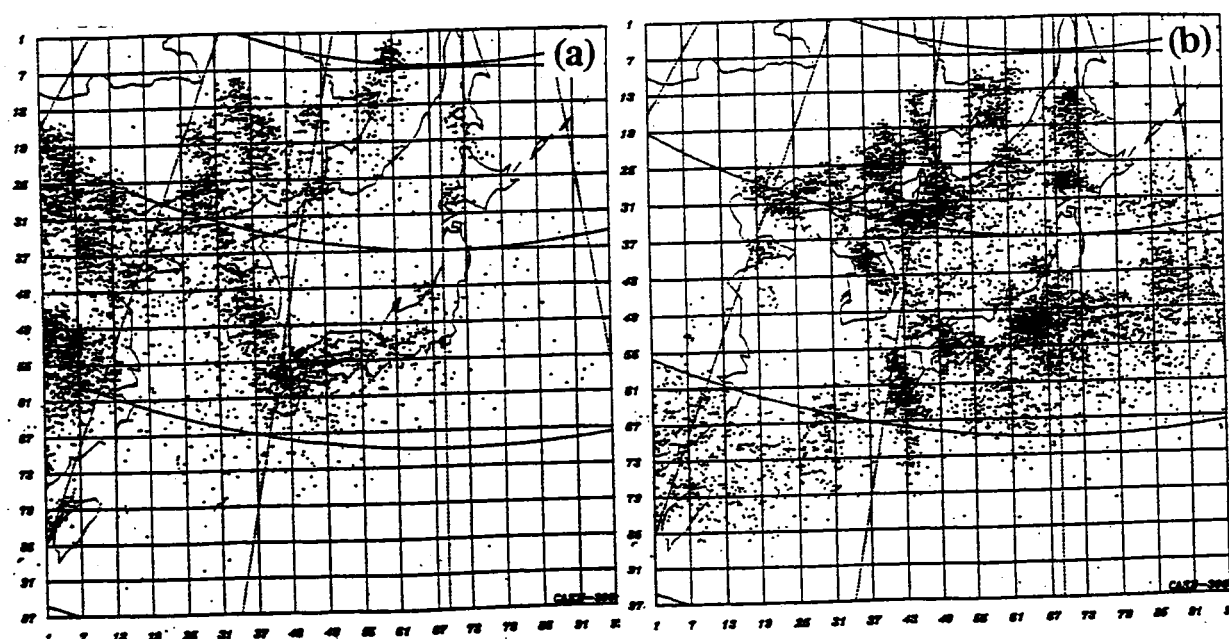

Fig. 4. Distribution of dry deposition (a) and wet deposition (b) during 5 days from 20th to 24th January 1985.

In the case of wet deposition, the distribution does not shown systematic because it only depends on the area of precipitation. Therefore, the long–range transport model requires to capture readily the precipitation. For this reason, we have been lavished much care on the meteorological submodel in present study. Furthermore, the meteorological submodel was sufficiently validated by using Geostationary Meteorological Satellite imagery and observed precipitation data.

On the other hand, horizontal distribution of dry deposition for 5 days from 13rd to 17th August 1985 is shown in Fig. 5(a). Contrary to prevail northwest wind in winter season, southerly wind prevailed during summer season, sulfur oxides are flown for the north direction around Japan because of weak southerly wind during the period. As a consequence, dry deposition also occurred relatively close to emission sources. As seen in Fig. 5(a), particles originated from Japanese emission sources deposited within the Japanese domestic region. But simulated wind field at 850 hPa level showed that the southerly wind changed to southwesterly center of the Sea of Japan by the effect of depression passed through Korean peninsula on 14th August and reached to the Sea of Okhotsk on 15th August. In consequence, wet deposition of sulfur oxides originated from emission sources in Japan occurred at the area from central part of the Sea of Japan to the Sea of Okhotsk as seen in Fig. 5(b).
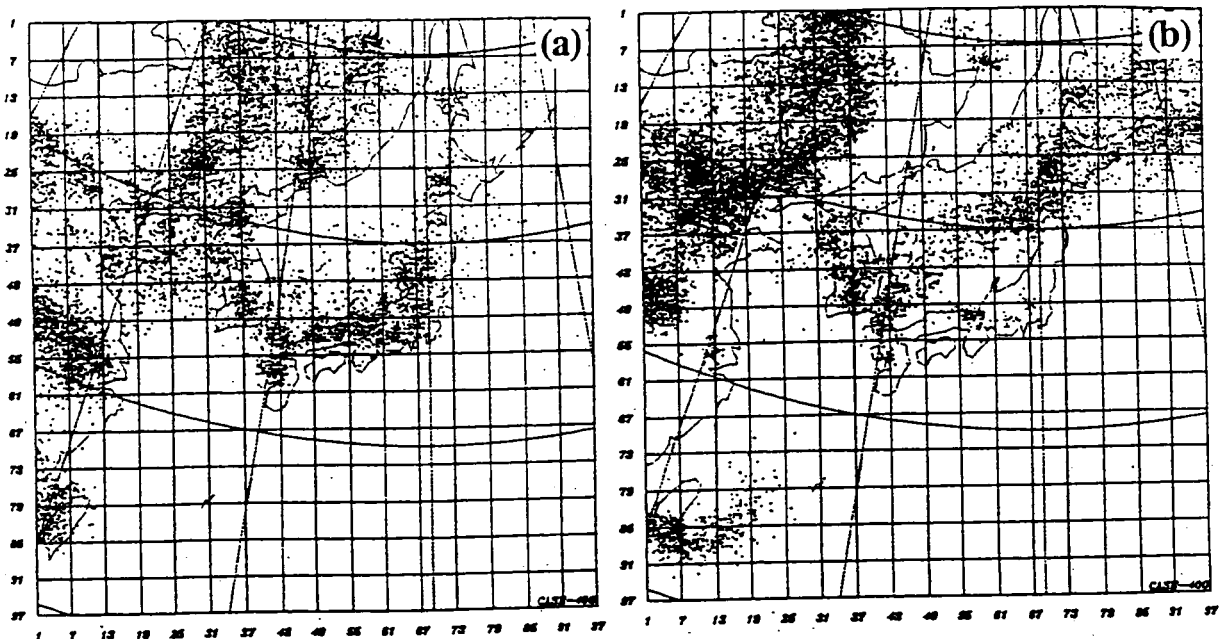
Fig. 5. Distribution of dry deposition (a) and wet deposition (b) during 5 days from 13rd to 17th August 1985.

3. Outline of the Model Results (National Insititue for Environmental Studies)

3.1 Numerical Model (STEM-II)

To understand the observed characteristics of long-range transport of pollutants, an atmospheric transport model which includes chemical reactions, the STEM-II (Sulfate Transport Eulerian Model; Carmichael et al[21], was applied. STEM-II is a three-dimensional Eulerian numerical model which accounts for transport, chemical conversion, and deposition of atmospheric pollutants. The major features of STEM-II include: emission of pollutants from point and area sources; transport by advection, convection, and turbulent diffusion; and spatially and temporally varying wind, temperature, pressure, water vapor, precipitation, and cloud fields.

The model treats chemical species in the gas, cloud, rain and snow phases. It includes mechanisms related to both cloudy and cloud-free environments, and in- and below-cloud wet removal and chemistry. For the gas phase chemical processes, the reaction mechanism of Lurmann et al.[22] was used.

STEM-II uses chemical, dynamic and thermodynamic parameterization, which allows for a wide variety of applications such as meso-, regional- and global scale air pollution studies. The code is modular in structure and can be driven by observed or modeled meteorological data. The dry deposition model proposed by Wesely[23] was used in the current application. A detailed description of STEM-II can be found inCarmichael et al.[21] In the present application, no precipitation or cloud processes were considered.

The East Asia model domain was a $1°$ latitude x $1°$ longitude grid system. The model domain covers from $110°$ E to $150°$ E and $20°$ N to $50°$ N. This horizontal domain is divided into a 41 x 31 mesh. The vertical model domain consists of 10 layers from ground level to 10,000 m. The vertical grid levels are 200, 400, 700, 1000, 2000, 3000, 4000, 5000,

7000, 10000 m. The model uses a terrain-following z* coordinate system. Figure 6 shows the model domain and field measurement sites.

The 1° latitude x 1° longitude gridded NO_x and SO_2 emission inventory reported by Akimoto and Narita[24] was used. The base year 1987 for NO_x and SO_2 emissions was used in this application. Emissions for far eastern Russia were not included. Nor where volcanic or other natural emissions. No seasonal or diurnal variation of emissions was considered. The yellow sand ("kosa") phenomenon also was not included in the model.

Piccot et al. (1992) have estimated global VOC (volatile organic carbon) emissions due to anthropogenic activities on a grid scale of 10° longitude by 10° latitude. Their data was used to prepare a regional scale VOC emissions

Figure 6   Calculation domain and field observation sites

inventory for the 1° x 1° grid domain shown in Figure 6. These 1° x 1 estimates were obtained by breaking down the larger scale emissions using population density (on a 1/3 degree scale) as the weighting factor. VOC category classes was re-classified into Lurmann et al.'s chemical reaction mechanism scheme. NO_x and VOC were emitted into the 1st and 2nd vertical levels, while SO_x was emitted into the 1st to 3rd levels.

All meteorological datasets were obtained from the Japan Meteorological Agency (JMA) Global Objective Analysis Data (GANAL) . The GANAL data consists of 12 hour interval 1.875° spatially gridded meteorological data points (wind speed and direction, temperature, dew-point temperature) at specified pressure levels. GANAL wind speed, temperature and humidity data were all interpolated into the 1° x 1° degree grid system shown in Figure 6. The 12 hour interval GANAL data were interpolated linearly in time space to generate an hourly interval meteorological data set.

3.2 Numerical Simulation Setting

Two high concentration episodes[26] were simulated. The first episode occurred from June 10 to June 26, 1991 and the second episode occurred from February 4 to February 28, 1992. The STEM numerical calculations were started with zero initial values except for O_3 (which was set 35 ppb through out the calculation domain).

The field observation details and results of basic analyses of the observed aerosol data have already been reported[26], therefore only a brief outline is given here. Aerosols were collected at three locations in Japan and Korea -- two urban sites (Ogori in Fukuoka prefecture, Japan and Seoul, Korea) and one rural site (Tsushima in Nagasaki prefecture, Japan). The Seoul and Ogori sites are located inland, while the Tsushima site is on an isolated island located in the strait between Japan and Korea. Figure 6 shows the monitoring locations. In this paper it was the observed data at Tsushima that was primarily used for analysis and comparison with numerical results. The monitoring site on Tsushima is located in a remote area with no residential structures within 2 km around the site. In addition, no large pollution source exist in the area. The elevation of the site is 380 m above sea level. Two high concentration episodes (June 1991 and February 1992) were observed during this series of
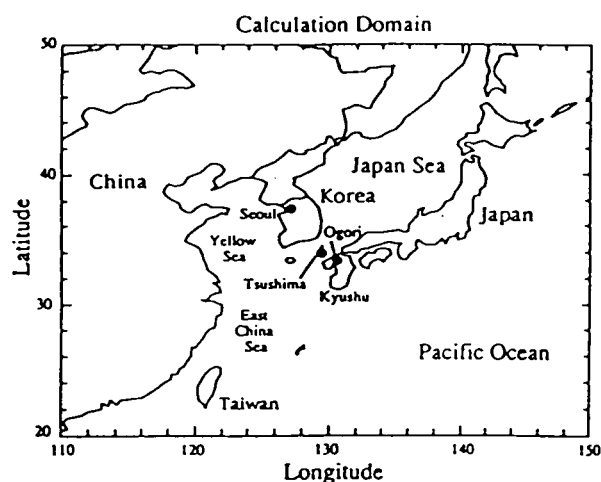
observations at the Tsushima site.

3.3 Analysis of June 1991 Episode

At the time of the June 1991 episode the rainy season meso-front stayed near the south edge of the Japan Islands from the beginning of June, and the wind convergence zone was observed along the meso-front lines. The wind speed of the northern part of this meso-front was relatively small and the air was stagnant. Precipitation was recorded on the 12th, 13th, 15th, 19-20th and 25-26th at Tsushima. (Heavy rain of 44 mm was recorded on the 13th. Except for this heavy rain, total precipitation was 14 mm).

Figure 7 shows the calculated distribution of SO_4^{2-} (μg/m^3) at z*=200 m level on June 22, 1991. The figure also includes the location of low / high pressure systems (L and H), the meso-front line (solid line for June 22 and broken line for June 21) , and the isentropic backward trajectories starting from Tsushima and Ogori (at z=1500 m level at 0900 JST). The trajectory line indicated by an open circle (o) starts from June 22 and that indicated by a cross (x) starts from June 21.

A high pollutant concentration region was simulated in the eastern part of China and southeast part of Korea. Pollution from this region was carried by winds from the Korean peninsula to the Korean Strait. The backward trajectory clearly indicates that the air mass observed at Tsushima was advected from a north - northwest direction. It shows that the trajectory calculated from June 22 passed over the high pollution concentration region.

Figure 8 compares model simulation results (line) and observation data (symbol) at Tsushima for SO_4^{2-} and NO_3^-. Model concentrations in the first vertical level were used in this plot. Arrows in the figure show the wind vector at z*=1000 m level. Figure 8 indicates that the STEM calculation successfully simulated the typical time variation of observed SO_4^{2-} concentrations. However, the model generally predicted sulfate concentration levels which were higher than observation data (overprediction was obvious from the 20th to 22th as can be seen in Figure 8). One highly plausible interpretation of this overprediction is the fact that the model ignores wet removal processes. Another is the fact
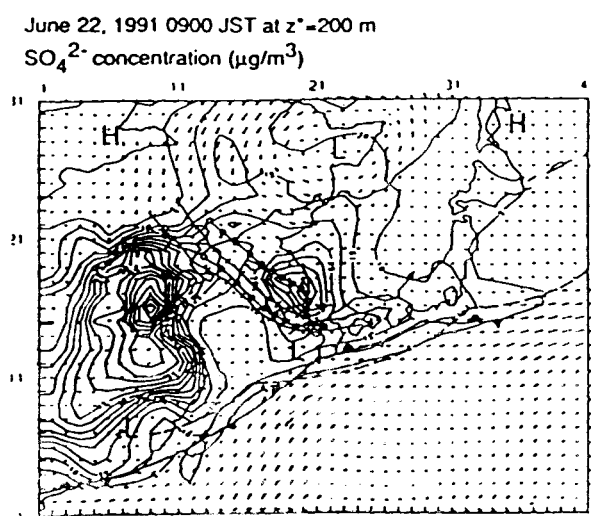
June 22, 1991 0900 JST at z*=200 m
SO_4^{2-} concentration (μg/m^3)

Figure 7 Aerosol sulfate (SO_4^{2-} concentration as simulated by STEM for June 22, 1991 at z*=200 m. H and L represent the location of major high and low pressure systems, respectively. Bold lines and broken lines indicate location of meso-front line for June 22 and June 21, respectively. Thin lines with symbols indicate isentropic backward trajectories calculated from Tsushima and Ogori, Japan at z=1500m. Open circles (o) indicate the trajectory calculated from June 22 and crosses (x) from June 21.
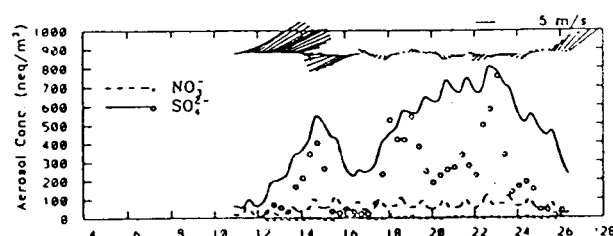
Figure 8 Comparison of observed data and model simulation results at Tsushima for June 1991. SO_4^{2-} and NO_3^- are plotted. Symbols indicate observed data and lines indicate calculated results.

that the spatial resolution is too coarse (the grid size is about 100 km horizontal; Figure 7 shows that there are sharp concentration gradients between Kyushu, Japan and the southern part of the Korean peninsula).

In general, simulated SO_4^{2-} concentrations display good agreement with observed levels. However, calculated HNO_3 concentrations are higher than observed NO_3^-.

It is clear from Figure 8 that the rainy season meso-front line plays an important role in the transboundary transport of pollutants. The calculated concentrations decrease after June 24 because the rainy meso-front moved north from the southern edge of the Japanese Islands to the northern part of Kyushu island.

3.4 Analysis of February 1992 Episode

At the time of the February 1992 episode measurements were conducted during what was typical winter monsoon conditions. A low pressure system moved from near the Taiwan area to east of the Japan Islands within the latitude range between 25° N - 30° N on the 10th-11th, 12th-13th and 22th-24th. After the passage of this low pressure system, a high pressure system slowly moved from the Yellow Sea to the Kyushu area. Total precipitation of 22 mm was recorded on 15th and 23th February at Tsushima.

Numerical simulation of the February 1992 episode is shown in Figure 9 for February 24. Figure 10 compares model simulation and observation data at Tsushima.

A sharp peak of aerosol SO_4^{2-} was observed on the 13th and 24th, and these periods were related to the passage of the low pressure system. The low pressure system and meso-front line movements shown in Figure 7 clearly indicate the transport of pollutants from the Asian mainland to the Yellow Sea and the Japan Sea direction, which occurred after the

Feb. 24, 1992 0900 JST at z*=200 m
SO_4^{2-} concentration $(\mu g/m^3)$
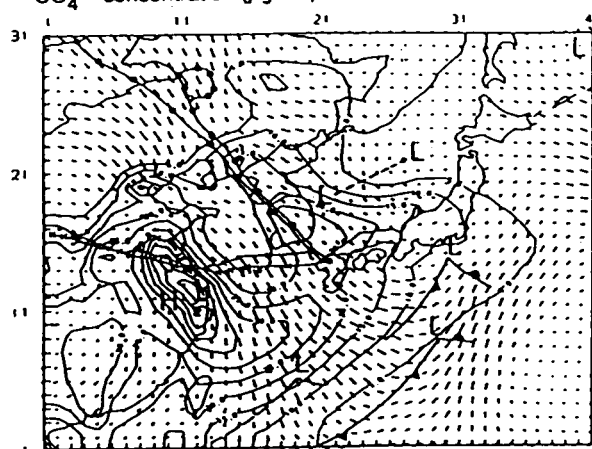
Figure 9   same as Figure 7 but for February 24, 1992.
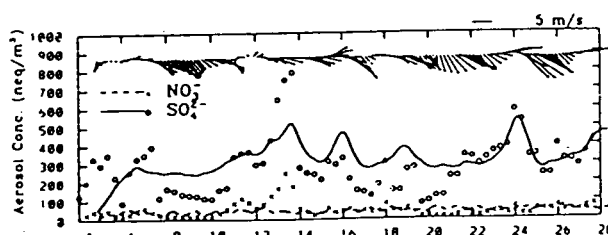
Figure 10   same as Figure 8 but for February 1992.

passage of the low pressure system and meso-front line. This fact indicates that the synoptic scale pressure system change play an important role in LRT in the East Asia region. Backward trajectories calculated from Tsushima clearly show that the pollutants were transported from the west, thus indicating trans-boundary transport.

Simulated SO_4^{2-} aerosol concentrations are shown in Figure 9. They generally trace the observed SO_4^{2-} concentration variation. (Note that simulation was started with zero initial concentrations, therefore the model values between February 4th and 6th should be understood as a warming up period for the simulation.) The magnitude of simulated and observed peak concentration values show good agreement (except for the peak on February 13th). However, the model values generally exceeded observed values. The concentrations of aerosol NO_3^-

show good agreement between observation and model values. This is not surprising because simulated HNO_3 simulates HNO_3 particulated into the aerosol state due to the low temperature conditions.

4. Concluding Remarks

In order to be skillful in the wet deposition process, the improvement of meteorological submodel to predict winds, clouds, and precipitation was carried out. Owing to get higher spatial resolution over focused area while keeping wider model domain such as the East Asian region, the JSM was nested within the FLM by using the spectral boundary coupling method. After the nested method was validated, the availability of the MRI long-range transport model was also validated by the test simulation of radioactive pollutants emitted from Chernobyl.

The Application run of the MRI-LTM was performed for the transport and removal of sulfur oxides over the East Asian region. Simulation was carried out for whole year of 1985, and adequate results were obtained.

Since the Lagrangian particle method was used in present model, it was possible to determine the source-receptor relations. The model is avail to investigate the impact for deposition originating from the continental emission sources.

Atmospheric transport model which includes chemical reactions, the STEM (Sulfate Transport Eulerian Model; Carmichael *et al*, 1986), was applied to the east Asia region. Extremely high pollutant concentration episodes observed at Tsushima in June 1991 and February 1992 were successfully simulated. The model reproduced the typical time variation of observed concentrations. Simulated spatial and time variation of the pollutants helped explain the observed concentration changes. It was found that wind pattern variations associated with a synoptic scale pressure system are extremely important for the transboundary long-range transport.

References

1. Hatakeyama, S., K. Murano, H. Bandow, F. Sasaki, M. Yamato and H. Akimoto, 1995: The 1991 PEACAMPOT air craft observation of ozone, NOx, and SO2 over the East China Sea, the Yellow Sea, and the Sea of Japan. *J. Geophys. Res.*, **100**, D11, 23143-23151.
2. Sato, J., T. Satomura, H. Sasaki and Y. Muraji, 1995: The long-range transport model with deposition and transformation components, and application to the East Asian region. *Proceedings of the 1st International Joint Seminar on the Regional Deposition Processes in the Atmosphere*. 158-172. Nov. 20-24, Seoul, Korea.
3. Hegg, D. A., P. V. Hobbs and L. F. Radke, 1984: Measurement of the scavenging of sulfate in clouds. *Atmos. Environ.*, **9**, 1939-1946.
4. Flossmann, A., 1991: The scavenging of two different types of marine aerosol particles calculated using a two-dimensional detailed cloud model. *Tellus*, **42B**, 463-480.
5. Sasaki, H., H. Kida, T. Koide and M. Chiba, 1995: The performance of long-term integration of a Limited Area Model with the spectral boundary coupling method. *J. Met. Soc. Japan*, **73**, 165-181.
6. Mellor, G. L. and T. Yamada, 1974: A hierarchy of turbulence closure models for planetary boundary layer. *J. Atmos. Sci.*, **31**, 1791-1806.
7. Satomura, T., F. Kimura, H. Sasaki, T. Yoshikawa and Y. Muraji, 1994: Numerical simulation of regional scale dispersion of radioactive pollutants from the accident at the Chernobyl nuclear power plant. *Pap. Met. Geophys.*, **45**, 51-63.
8. Tatsumi, Y., 1986: A spectral limited area model with time-dependent lateral boundary

condition and its application to a multi-level primitive equation model. *J. Met. Soc. Japan*, **64**, 637-663.

9. Ohno, H. and S. Isa, 1984: A statistical relation between GMS-viewed cloud amount and relative humidity. *Tenki*, **31**, 493-495. (in Japanese).

10. Stewart,D. A., R. E. Morris, M. K. Liu and D. Henderson, 1983: Evaluation an episodic regional transport model for a multi-day sulfate episode. *Atmos. Environ*, **17**, 1457-1473.

11. Waleck, C. J. R., R. A. Brost and J. S. Chang, 1986: SO2, sulfate and HNO3 deposition velocities computed using regional landuse and meteorological data. *Atmos. Environ.*, **20**, 949-964.

12. Eliassen, A. F. Hov, I. S. A. Isaksen, J. Saltbones and F. Stordal, 1982: A Lagrangian long range transport model with atmospheric boundary layer chemistry. *J. Appl. Met.*, **21**, 1465-1661.

13. Fisher,

14. Cox, R. A., 1974: Particle formation from homogeneous reactions of sulfur dioxide and nitrogen dioxide. *Tellus*, XXVI, 235-240.

16. Eliassen, A. and J. Saltbones, 1975: decay and transformation rates of SO2 as estimated from emission data, trajectory and measured air concentrations. *Atmos. Environ.*, **9**, 425-429.

17. Alkezweeny, A. J. and D. C. Powell, 1977: Estimation of transformation rate of SO2 to SO42- from atmospheric concentration data. *Atmos. Environ.*, **11**, 179-182.

17. Meagher, J. F. and E. M. Bailey, 1983: The seasonal variation of the atmospheric SO2 to SO42- conversion rate. *J. Geophys. Res.*, **88**, 1525-1527.

18. Satomura, T. and S. Yamada, 1992: Report of the Atmospheric transport model evaluation study workshop. *Tenki*, **39**, 71-73.

19. Kato, N., Y. Ogawa, T. Koide, T. Sakamoto, S. Sakamoto and Research Group on the Energy Consumption in Asia and Global Environment, 1991: Analysis of the structure of energy consumption and the dynamics of emission of atmospheric species related to the global environmental change (SOx, NOx and CO2) in Asia. NISTEP report, NO.21, 4th Policy-oriented Research Group, The National Institute of Science and Technology Policy (NISTEP), Science and Technology Agency of Japan. (in Japanese).

20. Sato, J., T. Satomura, H. Sasaki and Y. Muraji, 1995: The long-range transport model of sulfur oxides and its application to the East Asian region. *Technical Report of the Meteorological Research Institute*, No. 34, 1-101. (in Japanese)

21. Carmichael G.R.,Peters L.K. and Kitada T.(1986): A second generation model for regional-scale transport/ chemistry/ deposition, *Atmos. Environ.* , **20**, 173-188.

22. Lurmann,F.W., Lloyd, A.C., Atkinson, R. (1986): A chemical mechanism for use in long-range transport/acid deposition computer modeling, *J. Geophy. Res.*, **91**, 10905-10936.

23. Wesely,M.L. (1988): Imporved parametrizations for surfaces resistence to gaseous dry deposition in regional scal model, *EPA/6003-86/037* (PB86-218104).

24. Akimoto H. and Narita H.(1994): Distribution of SO_2, NO_x and CO_2 emissions from fuel combusition and industrial activities in Asia with 1° x 1° resolution, *Atmos. Environ.* , **28**, 213-225.

25. Piccot S., Watson S.D. and Jones J.W.(1992): A global inventory of volatile organic compound emissions from anthropogenic sources, *J. Geophys. Res.*, **97**, D9, 9897-9912.

26. Wakamatsu, S., A. Utsunomiya, J.-S. Han, A. Mori, I.Uno and K. Uehara: Seasonal variation in atmospheric aerosol concentration covering northern Kyushu, Japan and Seoul, Korea, *Atmos. Environ.* (submitted) 1995.